A FUZZY LOGIC APPROACH BASED DIRECT TORQUE CONTROL AND FIVE-LEG VOLTAGE SOURCE INVERTER FOR ELECTRIC VEHICLE POWERTRAINS

ABDELHAKIM DERBANE [1], BEKHEÏRA TABBACHE [1], AIMAD AHRICHE [2]

In this paper, a fuzzy logic approach is combined with direct torque control (DTC) for dual-motor based electric vehicle powertrain. The proposed structure is based on five-leg voltage source inverter (FLVSI) and two induction motors. The shared-leg switching-signals are selected by using a fuzzy logic controller in order to ensure an independent control of the two driving wheels. Indeed, the selection of the control sequence duration is performed based on the power demand and the load torque of each motor, Simulation results are carried out to confirm that both of IM is able to operate at different speeds with any load condition.

1. INTRODUCTION

Recently, electric vehicle technologies are becoming among the prominence solutions to replace the conventional systems which are based on the combustion. Therefore, multi-machine electric drives are widely used, and the enhancement of its performance becomes also an attractive task. In facts, many types of voltage source inverter (VSI) can be used to supply electric drives with independent control. For this case of dual three-phase ac-drive, at least two VSI's are required to supply the two motors. However, this structure leads to more complexity, high switching losses and a high number of power electronic components which presents the main drawback. To reduce the complexity and cost of these systems, another configuration based on single-inverter dual-motor is introduced [1–6]. The proposed solution uses only one parallel power VSI for the two induction motors. However, ensuring independent control is the main challenge for this approach. To overcome this problem, many inverter structures have been proposed in the literature. Most of them are aimed to minimize size, cost, and improve system efficiency [4]. In this context, five-leg voltage source inverter (FLVSI) is introduced. In this topology [5], one of the five-leg is shared by two induction motors, which can be also viewed as a degraded version of the conventional structure [6,7]. Moreover, in terms of control strategies, many advanced techniques are presented. Authors in [8] present a pulse width modulation (PWM) inverter based on (2n+1) legs associated with (n) electrical machines. Two main properties are shown for this topology; a constant switching frequency and the availability of dc bus voltage. In [9], PWM combined with an appropriate modification to generate modulated signals is proposed. The inverter switching frequency is minimized and kept equal for all inverter leg. In overall, FLVSI provides a saving of two switches, compared with the classical dual three-phase VSI. The current rating of the common leg has to be doubled. In [10], the authors describe an independent control drive of an electric vehicle, with two induction motors fed by FLVSI. Based on (DTC) associated with a speed control loop, the power conversion structure can be envisaged as a reliable backup solution in case of power inverter failure in classical powertrain based on three-phase inverters. This structure also comprises an electronic differential which by eliminating the

mechanical transmission increases the flexibility in the design, reduces the mass and the cost. In [11] two-arm modulations (TAM) technique is presented for independent control of two-induction motor drive fed by FLVSI. Two independent three-phase space vector modulators are utilized to control two motors. The experimental result indicates that the motor performance and voltage utilization factors of SVPWM are comparable with those of SPWM method. The similar voltage utilization factor in SVPWM is due to the TAM technique, which cancel-out the zero-vector signals in the modulation. Both techniques have similar capabilities in following various step speed demand operation and forward operation under the speed limit of FLVSI. In [12] predictive control of a two-motor drive with five-leg inverter is presented, the use of model predictive control (MPC) in the multi-machine drive has the advantages of independent fast current control of the machines, elimination of closed-loop system's cascaded structure. Prediction of future states is via the discrete-time model of the FLVSI and piecewise-affine model of two permanent magnet synchronous machines (PMSM). The use of MPC eliminates unfeasible switching states inherent in reduced-switch-count inverters while reducing computation and sampling times. In [13] finite-control-set model predictive control (FCS-MPC) combined with intrinsic characteristic of FLI has been elaborated, the required number of controllers is reduced from the conventional four to one predictive controller, and factor-tuning effort is saved. FCS-MPC provides faster transient performance and a good way to deal with the shared leg over current. Further on, [14] proposes a speed control scheme that minimizes the common leg current of FLVSI controlling two induction motors driven at the same speed, the speed control consists of two controllers, the first is an angle controller in the arm to have a constant phase angle difference between the two motors. The second is a slip controller that keeps the mechanical speed of the two motors the same when the load conditions are different. In [15] propose a current control of dual PMSM based on five-leg inverter, in this case the inverter can fully fulfill the vector space decomposition control of dual three-phase and has the same dynamical performance as the conventional dual three-phase VSI selection of phase from each set of signal three-phase windings as a pair to share the common leg, its current rating is approximately half of the rating of other legs. With

[1] Ecole Militaire Polytechnique, Alger, Algérie (e-mail: hakimderbane@gmail.com, laid_tabache@yahoo.com,).
[2] Laboratoire d'automatique appliquée, Université de Boumerdes, Boumerdes, Algérie, E-mail: Ahriche.a@gmail.com

the inverter non-linearity feed-forward compensation, the current unbalance could be mitigated in steady-state operation without deterioration of dynamical performance.

In this paper, the first section deals with state of art control of a five-leg inverter. The second section introduces direct torque control of FLI and presents the principle of independent control. The third section is dedicated to the fuzzy logic approach-based switching time selection. In Section 4, simulation results are carried out with different reference speeds and load torques, an alternative application of the sequences control is developed to drive both IM in an optimal way with the introduction of fuzzy logic. Section 5 present the application of fuzzy logic to the electric vehicle. Finally, a summary of the main ideas and performances is presented, and a conclusion closes the paper.

2. DIRECT TORQUE CONTROL OF FIVE LEG INVERTER FOR TWO INDUCTION MOTORS

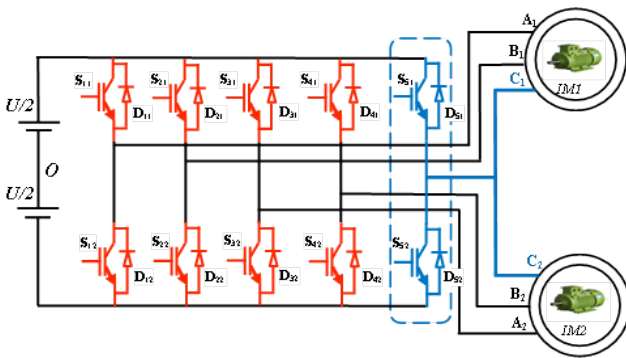Figure 1 shows the structure of the proposed system.

Fig. 1 – Five leg inverter for Dual-induction motors.

The line-to-neutral voltage equation is given by:

$$\begin{bmatrix} V_{A1} \\ V_{B1} \\ V_{C1} \\ V_{A2} \\ V_{B2} \\ V_{C2} \end{bmatrix} = \frac{U}{3} \begin{bmatrix} 2 & -1 & 0 & 0 & -1 \\ -1 & 2 & 0 & 0 & -1 \\ -1 & -1 & 0 & 0 & 2 \\ 0 & 0 & 2 & -1 & -1 \\ 0 & 0 & -1 & 2 & -1 \\ 0 & 0 & -1 & -1 & 2 \end{bmatrix} \begin{bmatrix} S_{11} \\ S_{21} \\ S_{31} \\ S_{41} \\ S_{51} \end{bmatrix} \quad (1)$$

The appropriate switching table of the five-leg inverter can be deducted from the conventional three-leg DTC. The control algorithm is based on the flux and torque hysteresis comparators, the stators-flux position. In overall, for five-leg inverter, 2^5 voltage vectors can be shown ($V_{i=1,.32}$ [S_1 S_2 S_3 S_4 S_5]; $S_{i=1,5}$ = either 0 or 1).

The control strategy should ensure a separate control of both induction machines. For that, the conventional DTC is adopted to synthesis the switching table. If the applied terminal-voltages of the third legs (V_{C1} and V_{C2}) are same, the problem doesn't arise. In the case where the voltage in the common leg is different ($V_{C1} \neq V_{C2}$), we give priority for one of them and applying a no-active voltage vector for the other. Thus, one of the two machines aren't driven in the optimal way, because of the application of no-active vectors. In addition, another drawback of the DTC-FLI is the peak value of the common-leg current which can be twice higher than the other legs.

To overcome these problems, an improved DTC-FLI

switching table is proposed. It is based on the alternative operating of one of the two machines in priority mode. Each machine (IM1 or IM2) has the priority only for half-sequence of the control time and during the remaining time; it operates in a degraded mode. However, with different active powers and load torques, dividing sampling time in twice isn't the optimal solution.

Among merits of the DTC control is the good performance when we reduce the sampling time. This advantage can be exploited to optimize the operating of the two machines based on their active powers and load torques. In fact, to determine the duration of the sequence control for each machine, more time should be given to the machine which has great power and torque. For that, we compare the instantaneous values of active power and load torque variation (ΔP, ΔT) in both machines. In this case, three states are distinguished

- (ΔP, ΔT) ≈ *0*, the sequence control is divided by two.
- (ΔP, ΔT) > *0*, IM1 has the priority.
- (ΔP, ΔT) < *0*, IM2 has the priority.

The switching table for the DTC-FLI is shown in Table 1.

3. FUZZY-LOGIC APPROACH BASED SWITCHING TIME SELECTION

In this section, fuzzy logic controller is designed to manage the operating duration of each motor. Otherwise, it allows the selection of the sequence control based on the values of power and torque. Since the small or great error between the active power and the load torque represents an uncertainty in our adopted strategy, the use of fuzzy logic (FL) approach offers better solution. For this, the switcher bloc is replaced by a fuzzy logic controller. Figure 2 gives the proposed fuzzy logic controller-based power management.
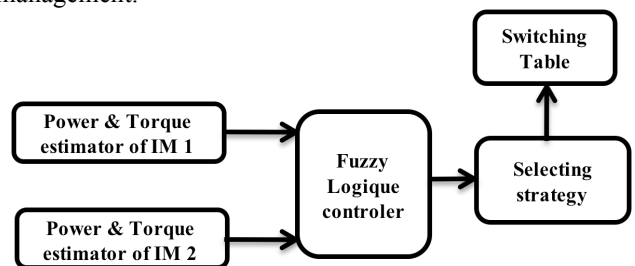

Fig. 2 – Scheme of fuzzy-based power management.

Two fuzzification inputs are used for our controller. The active power error (E_p) and load torque error (E_T) are given by the following equations:

$$E_p = \frac{P_1}{P_{1n}} - \frac{P_2}{P_{2n}}, \quad (2)$$

$$E_T = \frac{T_1}{T_{1n}} - \frac{T_2}{T_{2n}}, \quad (3)$$

where: P_1, P_2, T_1 and T_2 are the instantaneous values of active powers and load torques respectively, P_{1n}, P_{2n}, T_{1n}, and T_{2n} are the rated values of powers and torques of both machine.

Table. 1

Switching table of direct torque control for five-leg inverter

Cflx	C_{T1}=1 and C_{T2}=1	S1		S2		S3		S4		S5		S6	
		F1=1	F1=0	F1=1	F1=0	F1=1	F1=0	F1=1	F1=0	F1=1	F1=0	F1=1	F1=0
S1	F_2=1	V2	V18	V18	V17	V17	V25	V25	V9	V9	V10	V10	V2
	F_2=0	V6	V22	V22	V17	V17	V25	V25	V9	V9	V14	V14	V6
S2	F_2=1	V6	V22	V22	V17	V17	V25	V25	V9	V9	V14	V14	V6
	F_2=0	V8	V24	V24	V21	V21	V29	V29	V13	V13	V16	V16	V8
S3	F_2=1	V8	V24	V24	V21	V21	V29	V29	V13	V13	V16	V16	V8
	F_2=0	V8	V24	V24	V23	V23	V31	V31	V15	V15	16	V16	V8
S4	F_2=1	V8	V24	V24	V23	V23	V31	V31	V15	V15	V16	V16	V8
	F_2=0	V8	V24	V24	V19	V19	V27	V27	V11	V11	V16	V16	V8
S5	F_2=1	V8	V24	V24	V19	V19	V27	V27	V11	V11	V16	V16	V8
	F_2=0	V4	V20	V20	V17	V17	V25	V25	V9	V9	V12	V12	V4
S6	F_2=1	V4	V20	V20	V17	V17	V25	V25	V9	V9	V12	V12	V4
	F_2=0	V2	V18	V18	V17	V17	V17	V25	V9	V9	V10	V10	V2
C_{T1}=1, C_{T2}=0		V8	V24	V24	V17	V17	V25	V25	V9	V9	V16	V16	V8
C_{T1}=0, C_{T2}=1		V26	V30	V30	V5	V5	V7	V7	V3	V3	V28	V28	V26
C_{T1}=0, C_{T2}=0		V32	V32	V32	V32	V32	V32	V32	V32	V32	V32	V32	V32

The fuzzification is performed by using singleton fuzzifier. We define two types of membership function corresponding to two variable inputs as illustrated in Fig. 3.
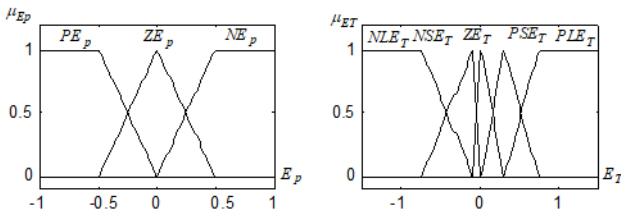

Fig 3 – Membership function of fuzzy variables inputs.

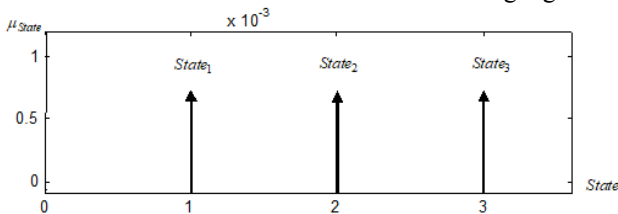The control variable is the state of the common leg Fig. 4.

Fig. 4 – Membership function of fuzzy variables outputs.

It can be seen that the power and torque errors have relative values. The motor that has larger errors is selected and defined as Master. Thus, the switcher bloc selects the appropriate switching vector of the motor DTC. With the same analysis, the motor with the smaller errors is defined as Slave. From the above figure, it can be seen that three switching states are chosen. Each control rule can be described using E_p, E_T and the control variable. The rule Ri is given as:

Ri: if Ep is Ai and E_T is Bi then N is Ni

where: Ai, Bi, and Ni represent the fuzzy segments.

The inference method is based on the minimum operation rule as a fuzzy implementation function. The membership function of Ai, Bi, and N are given by μ_A, μ_B, and μ_N respectively. The ith rule α_i can be expressed as:

$$\alpha_i = \min\left(\mu_{A_i}(E_p), \mu_{B_i}(E_T)\right) \qquad (4)$$

By using Mamdani's minimum operation rule as a fuzzy implication function, the ith rule leads to the following control decision:

$$\mu_{Nl}(n) = \min(\alpha_i, \mu_{Ni}(n).) \qquad (5)$$

Thus, the membership function μ_N of the output N is:

$$\mu_N(n) = \max_{i=1}^{3}\left(\mu_{Ni'}(n)\right). \qquad (6)$$

Since the output is crisp, the maximum criterion method is used for defuzzification. The value of fuzzy output which has the maximum possibility distribution is used as a control output.

4. **RESULTS AND DISCUSSION**

To illustrate performances of the proposed control, simulations are carried out with two induction motors. For that, different load torques, and reference speeds are tested to perform the independent control. The flux reference value is set to 1.2 Wb for both induction motors. Firstly, both of IM1 and IM2 are operated with no-load and under different load torques and same rotation speeds in order to prove the effectiveness of the proposed algorithm.

Figures 5 and 6 show the line-to-line terminal voltages in both motors.

In Fig. 9, the evolution of IM1 and IM2 electromagnetic torques are given respectively by the blue and red lines. From 0 to 2 seconds, the motors are run with no-load at 5 Hz. from 2 to 4 seconds for the IM1 is run under 6 N.m load torque and IM2 under 5 N.m with the same speed (5 Hz). This same figure illustrates also the performances when using independent control.
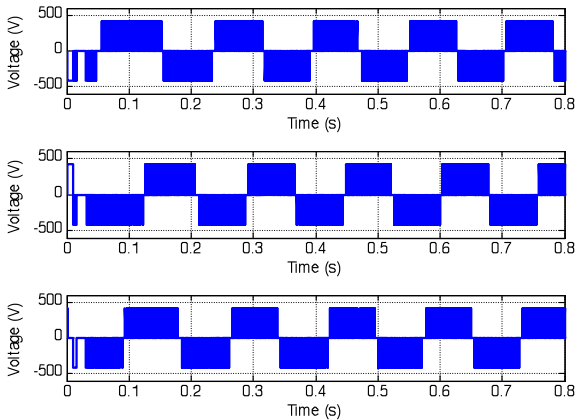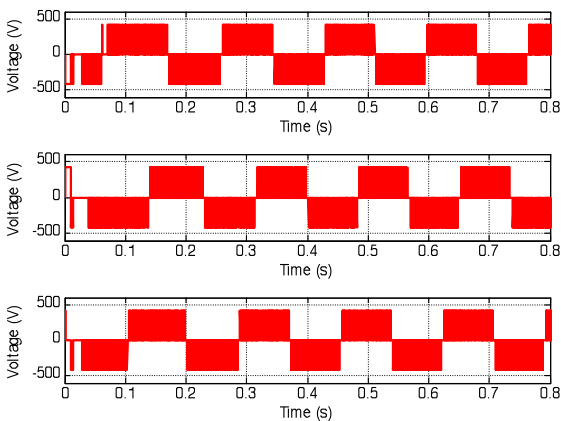

Fig. 5 – Line-to-line voltage of IM1.

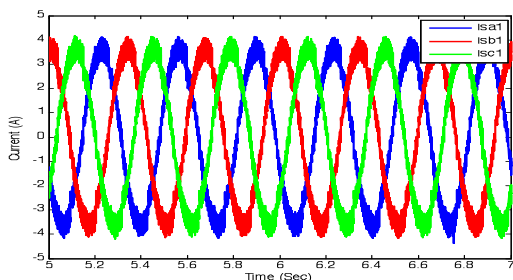Fig. 6 – Line-to-line voltage of IM2.
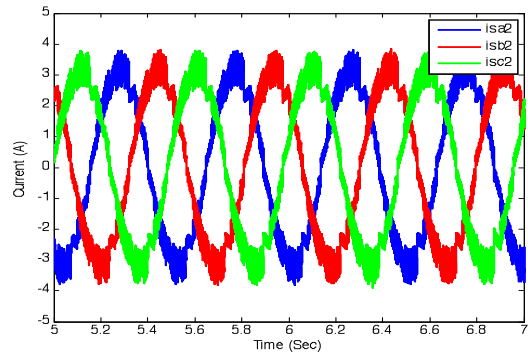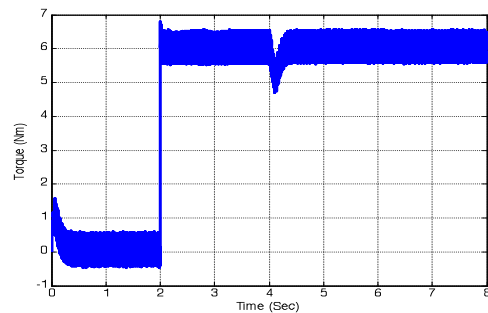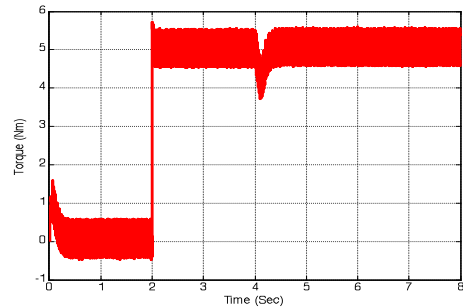

Fig. 7 – Line current of IM1.

Fig. 8 – Line current for IM2.

a) IM1: Electromagnetic torque.

b) IM2: Electromagnetic torque

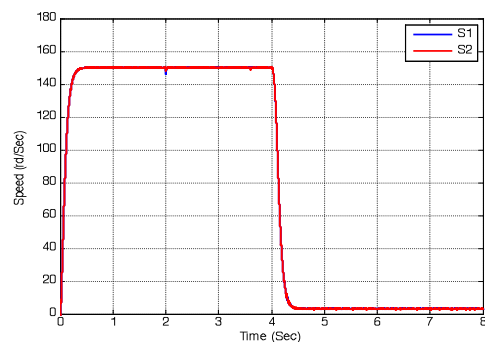Fig. 9 – Evolution of torque in IM1 and IM2 respectively.

Fig. 10 – IM1 and IM2 Speeds.

Figures 7 and 8 show that both of induction motors absorb a sinusoidal current. Figure 10 illustrates the induction motor performance in term of speed. IM1 and IM2 speeds are given respectively by the blue and red lines. It is well shown that the reference speed is tracked perfectly.

Figure 11 gives the current response in the common leg of five-leg inverter in the case of the same reference speed. In this case, the common leg provides sinusoidal current where the amplitude is equal two times of each induction motor current with the same frequency.

Figures 12 and 13 show the shared leg current with different references speed. It can be concluded that the proposed independent control based on direct torque control gives a promising performance in term of speed and flux.
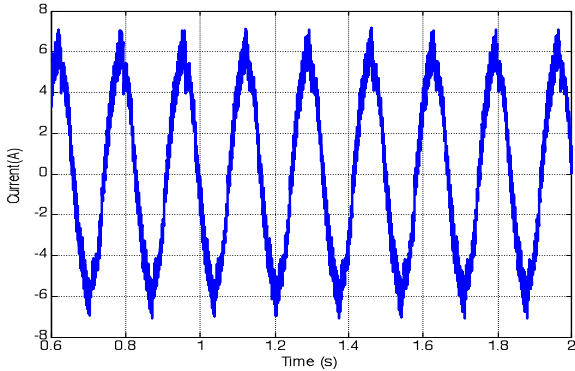

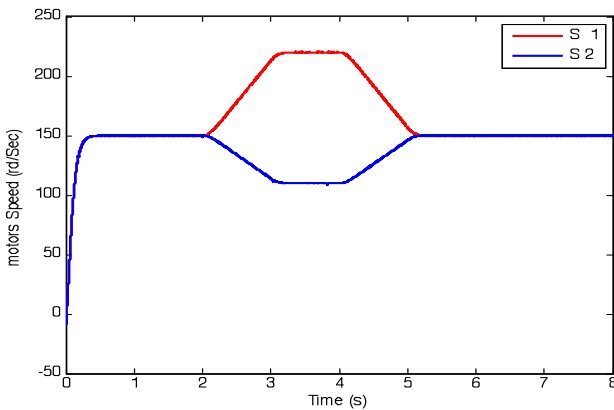Fig. 11 – Common leg current with the same speeds.

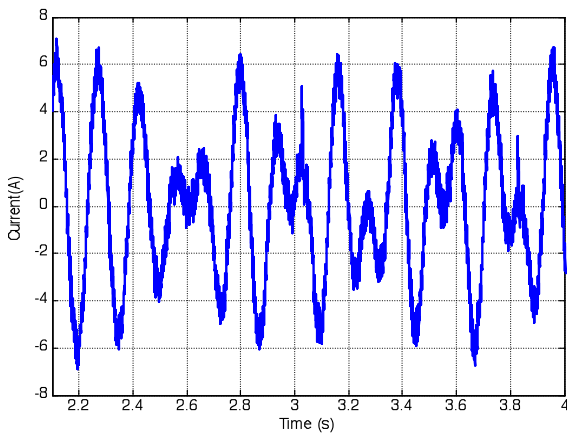Fig. 12 – Speeds of both induction motors.

Fig. 13 – Common leg current with different speeds.

5. ELECTRIC VEHICLE APPLICATION

For driving-wheels in classical configuration of EV, the two induction motors are powered by two separate three-phase VSI's. Nevertheless, in faulty mode operation (for example fault in IGBT's), we opted for a FLI to supply the system in order to keep powered the EV.

On the other hand, it is also possible to use the five-leg inverter for powertrain to reduce the number of power components, and thus reduce the cost of the system.
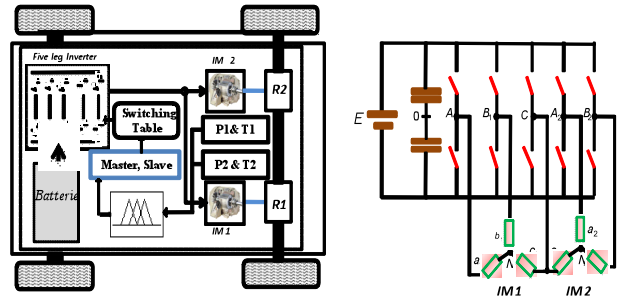

Fig. 14 – Electric vehicle fed by FLI with fuzzy logic.

The proposed strategy takes into account the EV aerodynamics. Thus, the given vehicle model is based on mechanics and aerodynamics principles [10]. The proposed configuration of EV is given in Fig. 14.

In order to test the performance of the electric differential, numerical simulations were performed on an electric vehicle powered by two asynchronous motors of 37 kW. The electric vehicle will be represented by its dynamic model, whose characteristics are given in the Appendix.

In the simulation below Fig. 15, the resistant forces generated by the vehicle's dynamic model represent the load torque of the two motors through the gearbox and the wheel radius. To test the decoupled control of the two driving wheels with the application of the electric differentiator, we have considered the following scenario:

At start-up, we consider a straight trajectory whose two engines have the same speed. Between $t = 140$ s and $t = 162.5$ s, a right turn of 45° was simulated. Then the vehicle will continue a straight trajectory until $t = 800$ s. At this time, we apply a left turn of 30° to $t = 900$ s. Finally, the vehicle will continue on a straight path until the end of the cycle. In this case, we apply as a reference speed a European standardized driving cycle (NEDC: New European Driving Cycle).

In the case of a rectilinear trajectory, both motors react in the same way in terms of speed and torque. In the event of a turn, the electric differential distributes the appropriate references to the two engines in order to ensure the stability of the vehicle. In both cases (rectilinear or bend) the linear speed of the vehicle remains constant.
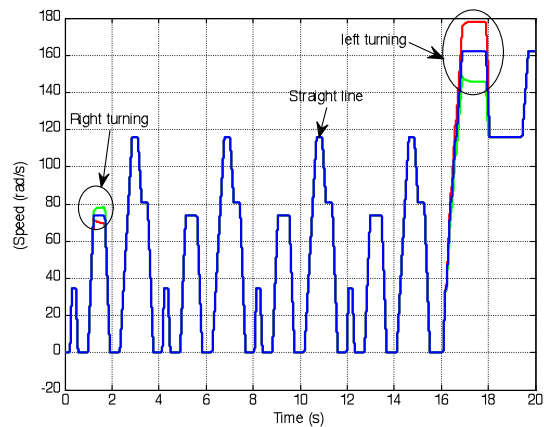

Fig. 15 – Electric vehicle speeds .

The right engine speed in blue and the left engine in red. The green curve represents the linear speed of the vehicle. Simulation results confirm the independent control of the two motors by a five-Leg inverter. In steady state, we can see that the current of the two motors is sinusoidal.

In addition, the current of the common leg is distorted because of the difference in speed of the two motors. In the case where the two motors operate at the same speed, the current of the common leg has a sinusoidal shape and it is doubled compared to the other phases.

6. CONCLUSION

In this paper, a fuzzy logic approach-based DTC-FLI control is introduced for an electric drive. The proposed method is performed in order to ensure an independent control of two induction motors by means a five-leg inverter. For this, a common neutral point-based structure of five-leg voltage source inverter is illustrated. The selection of switching signals is done based on the well-known DTC control strategy. The whole algorithm is verified under various driving cycles with an electric vehicle. Validation results are shown and discussed in order to verify the feasibility and the robustness of the proposed system.

APPENDIX

Induction motors parameters:

Rated data of the simulated motor
$P_N = 0.9$ kW, $\Omega_N = 1440$ rpm, $p = 2$
$R_s = 1.823\ \Omega$, $R_r = 22.63\ \Omega$, $X_{Ls} = 56.3\text{e-3}\ \Omega$
$X_{Lr} = 84.6\text{e-3}\ \Omega$, $X_{Lm} = 996.3\text{e-3}\ \Omega$
$J = 0.05$ Kg.m².

Rated data of the simulated motor for EV
M_2: $P_N = 37$ kW, $\Omega_N = 1480$ rpm, $p = 2$
$R_s = 0.0851\ \Omega$, $R_r = 0.0658\ \Omega$
$L_s = 0.0314$ H, $L_r = 0.0291$ H, $L_m = 0.0291$ H,
$J = 0.37$ Kg.m², $k_f = 0.02791$ Nm.sec

REFERENCES

1. W. Wang, J. Zhang, M. Cheng, *A dual-level hysteresis current control for one five-leg VSI to control two PMSMs*, IEEE Trans. Power Electron., **32**, *1*, pp. 804-814 (2017).
2. F. Korkmaz, I. Topaoglu, H. Mamur, *Fuzzy logic Based Direct torque control of Induction Motor with Space Vector Modulation, IJSCAI*, **2**, *5/6* (2013).
3. R. Hemantha Kumar, A. Iqbal, N. C. Lenin, *Review of recent advancement of direct torque control in induction motor drives – a decade of progress, IET Power Electronics*, **11**, *1*, pp. 1-15 (2017).
4. S. Gdaim, A. Mtibaa, M. F. Mimouni, *design, Experimental Implementation of DTC of Induction Machine based on Fuzzy logic control on FPGA*, IEEE Trans. on Fuzzy System 10.1109/TFUZZ (2014).
5. Y. Mei, S. Feng, *An optimized Modulation Method for a Five-Leg – Inverter for dual Induction Motor Drives*, IEEE 978-1-5090-1210 (2016).
6. R. Isermann, *On fuzzy logic application for automatic control, supervision, and fault diagnosis*, IEEE Trans. Systems, Man and Cybernetics-Part A: Systems and Humans, **28**, 2, pp. 221-235 (1998).
7. M. S. Ballal et al., *Adaptive neural fuzzy inference system for the detection of inter-turn insulation and bearing wear faults in induction motor*, IEEE Trans. Industrial Electron., **54**, *1*, pp. 250-258, (2007).
8. D. Dujić, M. Jones, S. Vukosavic, E. Levi, *A general PWM method for a (2n+1)-leg inverter supplying n three-phase machines*, IEEE Trans. Ind. Electron., **56**, *10*, pp. 4107–4118 (2009).
9. M. Jones, S. N. Vukosavic, D. Dujić, E. Levi, P. Wright, *Five-leg inverter PWM technique for reduced switch count two-motor constant power applications*, IET Elect. Power Appl., **2**, *5*, pp. 275–287 (2008).
10. B. Tabbache, S. Douida, *Direct torque control of five-leg inverter dual induction motor powertrain of electric vehicles*, Electr. Eng., **99**, pp. 1073-1085 (2017).
11. M. Talib, Z. Ibrahim, N. Rahim, A. Hasim, *Implementation of space vector two-arm modulation for independent motor control drive fed by a five-leg inverter*, J. Power Electron, **14**, *1*, pp. 115–124, (2014).
12. C. S. Lim, N. Abd Rahim, W. P. Hew, E. Levi, *Model predictive control of a two-motor drive with five-leg-inverter supply*, IEEE Trans. Ind. Electron., **60**, *1*, pp. 54–65 (2013).
13. D. Zhou, Jin Zhao, Y. Li, *Model Predictive Control Scheme of Five-Leg AC-DC-AC Converter-Fed Induction Motor Drive*, IEEE J. Trans. on Ind. Electronics, **63**, *7*, pp. 4517–4526 (2016).
14. Y. S. Lim, J.-S. Lee, K. B. Lee, *Advanced Speed Control for Five Leg Inverter Driving a Dual-Induction Motor System,* IEEE Trans. on Ind. Electronics, 0278-0046 (2018).
15. Y. Hu, S. Huang, X. Wu, X. Li, *Control of dual three-Phase Permanent Magnet Synchronous Machine Based on Five-Leg Inverter*, IEEE Trans. on Power Electronics (2019).
16. V. Naik N, S. P. Singh, *A Two-Level Fuzzy Based DTC Using PLLC to Improve the Induction Motor Performance,* IEEE (2016).
17. B. Tabbache, M. Benbouzid, A. Kheloui, J.-M. Bourgeot, A. Mamoune, *An Improved Fault-Tolerant Control Scheme for PWM Inverter-Fed Induction Motor-Based EVs*, ISA Trans., **52**, pp. 862-869, (2013).
18. C. Xia, J. Zhao, Y. Yan, T. Shi, *A Novel Direct Torque Control of Matrix Converter-Fed PMSM Drives Using Duty Cycle Control for Torque Ripple Reduction*, IEEE Trans. on Ind. Electron., **61**, pp. 2700-2713, June (2014).
19. A. Khodadoost, A. Radan, *Novel comparative study between SVM, DTC, and DTC-SVM in Five-Leg Inverter to drive two motors independently*, in Proc. 4th Power Electronics, Drive Systems, and Technologies Conference, pp. 294 – 300 (2013).
20. D. Zhou, J. Zhao, Y. Li, *Model Predictive Control Scheme of Five-Leg AC-DC-AC Converter-Fed Induction Motor Drive*, IEEE J. Trans. on Ind. Electronics, **63**, *7*, pp. 4517–4526 (2016).
21. M. Talib, Z. Ibrahim, N. Rahim, A. Hasim, *Analysis on speed characteristics of five-leg inverter for different carrier-based PWM scheme,* Proc. IEEE Int. Power Engineering Optimization Conference (PEOCO), pp. 96–101 (2012).
22. M. Talib, Z. Ibrahim, N. Rahim, A. Hasim, *Characteristic of induction motor drives fed by three legs and five-leg inverter*, J. Power Electron., **13**, *5*, pp. 806–813 (2013).
23. W. Wang, M. Cheng, B. Zhang, Y. Zhu, *A fault-tolerant permanent-magnet traction module for subway application*, IEEE Trans. Power Electron., **29**, *4*, pp. 1646–1658 (2014).
24. C. S. Lim, E. Levi, M. Jones, N. Abd. Rahim, W. P. Hew, *A fault-tolerant two-motor drive with FCS_MP based flux and torque control*, IEEE Trans. Ind. Electron., **61**, *12*, pp. 6603–6614 (2014).
25. P. Raja Reddy, B. M. Manjunatha, D. V Ashok Kumar, *Five Leg Z-source Inverter Feeding Two Independent Loads Simultaneously*, Int. J. Advanced Res. Electr. Electron. and Instrum. Eng., **3**, *9* (2014).
26. A. Essalmi, H. Mahmoudi, A. Abbou, A. Bennassar, *DTC of PMSM based on artificial neural networks with regulation speed using the fuzzy logic controller,* IEEE (2014).
27. J. S. Lee, K.-B. Lee, *An open-switch fault detection method and tolerance controls based on SVM in a grid-connected T-type rectifier with unity power factor*, IEEE Trans. Ind. Electron., **61**, *12,* pp. 7092–7104 (2014).